Available online at www.sciencedirect.com
SCIENCE DIRECT
Journal of Sound and Vibration 293 (2006) 299–319
JOURNAL OF SOUND AND VIBRATION
www.elsevier.com/locate/jsvi

Assessment of nonlinear distortions in modal testing and analysis of vibrating automotive structures

P. Verboven, P. Guillaume, S. Vanlanduit*, B. Cauberghe

Department of Mechanical Engineering, Vrije Universiteit Brussel, Acoustics and Vibration Research Group, Pleinlaan 2, B-1050 Brussels, Belgium

Received 9 December 2003; received in revised form 25 May 2005; accepted 30 September 2005
Available online 24 February 2006

Abstract

In this paper, new developments for the nonparametric processing of modal test data are presented. Classically, random noise signals are applied to deal with possible nonlinear distortions during frequency response function measurements of linear dynamic systems. However, the use of multisine excitation signals allows the engineer to control much more his experiments. First of all, the nonparametric estimation of multivariable frequency response functions can be more easily based on an "errors-in-variables" stochastic framework. In addition, the application of a well-chosen multisine excitation permits improvement of the data quality, as well as the detection, qualification and quantification of nonlinear distortions during FRF measurements. To make the presented techniques available for multi-input modal testing, attention is paid to the design of optimal multi-input excitations by maximizing the Fisher information matrix as well as minimizing the crest factor of the applied excitation.

1. Introduction

In a limited amount of cases it is not possible, or very difficult, to control, or even to measure, the excitation forces acting on the structure under test (bridges excited by traffic and wind, operating machines, etc.). In most modal analysis applications, however, the excitation forces can be imposed with an actuator, and the engineer can choose which excitation signal to use.

A common way of measuring Frequency Response Functions (FRF) in the 1960s consisted in using slowly varying swept sine excitations together with tracking filters. With the development of signal processing techniques, such as the Fast Fourier Transform (FFT), it became possible to use broadband excitation signals [1]. This resulted in a considerable reduction of the measurement time, but also in important additional errors (such as leakage and aliasing) if no precautions were taken.

One way to avoid these errors consists in using periodic excitation signals such as multisines, which will also be used throughout this paper. Besides avoiding spectral errors, multisines offer other advantages such as optimal signal-to-noise (SNR) ratios, and a reduction of the number of periods required for averaging during the nonparametric identification of the FRF matrix (nonparametric stands for describing the dynamics of the

*Corresponding author. Tel.: +32 2 629 2805; fax: +32 2 629 2865.
E-mail address: svlandui@vub.ac.be (S. Vanlanduit).

0022-460X/$ - see front matter © 2006 Elsevier Ltd. All rights reserved.
doi:10.1016/j.jsv.2005.09.039

observed system by its spectral contents i.e. a transfer function). In addition (as will be discussed in Section 3) a synchronized set-up, with deterministic excitation using e.g. multisines, permits the use of a maximum likelihood FRF estimator developed in a "errors-in-variables" (EV) stochastic framework. As will be shown, such an estimator outperforms the traditionally-used FRF estimators such as the H_1 and H_v [2].

Modal testing of large structures, typically encountered in the automotive and aerospace industries, certainly requires the use of multi-shaker excitation. Very early, the possibility offered by exciting multi-input systems with uncorrelated signals has been investigated. The most obvious approach consists in applying independent random noise sources to the different inputs of the system (see for instance Ref. [3]). In Ref. [4] the design of uncorrelated binary sequences was studied. Nowadays, it is possible to generate more sophisticated signals, such as multisines for instance, which offer a lot of flexibility to the test engineer [5]. In this paper an excitation scheme for multisines will be considered only needing the design of a single multisine in the frequency band of interest. This excitation scheme (cf. Section 4.2) is optimal in the sense that it optimizes the Fisher information matrix for amplitude constrained inputs.

However, besides reducing the measurement time and improving the quality of the FRF data, the effects of possible nonlinear distortions become even more important. For this reason, most engineers still prefer the use of random noise excitation, since the contribution of nonlinearities is expected to be reduced by the averaging of random noise sequences. Nevertheless, the ideal FRF measurement method should not only provide accurate FRFs, but at the same time the presence of nonlinear distortions should be known to the engineer in order to properly judge the suitability of the FRF data for a subsequent modal analysis, which in the end is based on linear assumptions. It will be shown in this paper how the use of specially selected periodic excitation signals extends the engineer's possibilities to detect, qualify and quantify nonlinear distortions, which can have a large impact on the further modelling results if not recognized. Recently, new developments for this purpose have been presented for single input single output systems based on the use of multisines [6–10].

For cases where the typical input amplitudes clearly distort the structure's linear behaviour (e.g. a high level of operational input amplitudes) efficient nonlinear frequency analysis tools are available [11–13]. However, this paper aims at proposing additional tools to assess the level of distortions when one wants to use a modal analysis approach. In the end, modal-based analysis and design have become an integrated part in the automotive research and development process. Engineers appreciate the strong relation between the models and physics of structures and often use modal-based optimization tools that were developed in the recent years.

As a summary, this paper generalizes recently developed multisine-based SISO techniques to multivariable modal testing, where the aspects of multi-input experiment design, "errors-in-variables" nonparametric processing and the assessment for nonlinear distortions during testing are combined in an advanced modal test procedure. More specifically, the following contributions will be discussed:

- the maximum likelihood estimation of multivariable FRFs and their noise covariance matrix from MIMO multisine measurements when using a synchronized measurement setup.
- the optimization of multi-input excitation in modal testing, simply by the use of one single multisine realization based on an excitation scheme that maximizes the so-called Fisher information matrix.
- the practical assessment of the recently developed multisine-based methods for the detection and characterization of nonlinear distortions for mechanical structures and the generalization of these tools to MIMO modal testing.
- illustration of the benefits and at the same time ease-of-application of the different tools that were integrated in a multivariable modal testing procedure by means of experimental results for an application in the field of vibration analysis for automotive engineering.

2. Class of multisine signals

A multisine is a periodic broadband signal consisting of a sum of (co-)sines with harmonically related frequencies

$$s(t) = \sum_{k=1}^{F} A_k \cos(2\pi k f_0 t + \phi_k). \tag{1}$$

The period of the signal is $T = 1/f_0$. The amplitudes, A_k (k harmonic numbers) of the (co-)sine can be chosen arbitrarily while the phases ϕ_k are usually selected in such a way that the crest factor (i.e. the ratio of the peak and effective (RMS) value) is minimal. The amplitudes completely determine the auto-power spectrum of the signal, while the phases influence the peak value of the signal. Multisine can be considered as a generalization of stepped sine measurements. Stepped sine frequency response measurements are usually characterized by very good signal-to-noise ratios but long measurement times. Multisine makes it possible to reduce the measurement time while maintaining good SNRs [14].

By replacing classically-used random noise by multisine signals the user gets additional advantages:

- Leakage errors are avoided when properly used (i.e. synchronized measurements of an integer number of periods).
- The amplitude spectrum A_k is deterministic, resulting in a better SNR behavior, especially for a small number of averages/realizations.
- A full control over the amplitude spectrum is obtained such that it is possible to focus all the power in a desired frequency band, or to avoid the excitation of specific frequency bands or lines.
- In addition insights in the presence of nonlinear distortions can be obtained, e.g. the level of the even and odd nonlinear distortions can be separated, at the cost of an increased measurement time (factor 2 for odd to 4 or odd–odd multisines).

3. Multivariable "errors-in-variables" frequency response measurements

The nonparametric estimation of FRFs (or impulse response functions) is of primary importance in many scientific investigations. This is the reason why much attention has been paid to nonparametric estimators in the literature [3,15–17,2]. Most estimators, however, only consider the errors on the output measurements, not the input errors. In many practical situations, however, the disturbances on the input measurements can become as large as the ones on the outputs.

The reason for using an EV framework relates to a typical modal test setup, where there exists a permanent fixation, a so-called stinger, between the electrodynamic shakers and the structure. Such a stinger, having a high stiffness in the longitudinal direction while being flexible in the transversal direction, serves as a interface to ensure that the forces are applied perpendicular to the structure. As a result, around the resonance frequencies of the structure, the structure will resist additional input of energy resulting in low levels of the applied force and consequently higher noise levels on the input (force) Fourier data. Practically this means that the SNR drops at the resonance frequencies and one can certainly not assume that the applied force is free of errors. This is certainly not in favour of the H_1 FRF estimator, which requires that the input noise must be negligible in order to avoid biased FRF estimates. Therefore, it is certainly beneficial to work in an EV framework, which is in the case of arbitrary excitation (e.g. random noise) possible by the use of an *instrumental variables* (IV) method (see for instance Refs. [18,19]). The IV method usually requires an additional data sequence (i.e. the instrumental variables) which can be considered as a drawback. A positive result is the fact that, under some mild conditions, the IV estimate can be proven to be strongly consistent. Another possibility is to use the H_v estimator, which relies on the total least squares method. The H_v estimates are (statistically) consistent when the input/output errors are all equally large and uncorrelated, which is often not the case in practice. Then, consistent estimates can still be obtained by introducing a scaling matrix resulting in a generalized total least squares problem [20]. To derive this scaling matrix, however, the "true" covariance matrix of the input and output errors should be a priori known. In the next two sections the nonparametric estimation of FRFs will be revisited for multisines taking into account the specific aspects of periodic excitations, i.e. the availability of repeated observations within a synchronized setup.

3.1. Problem formulation

Consider the multivariable system with N_i inputs and N_o outputs as shown in Fig. 1. If the "true" input and output signals, $f_0(t) \in \mathbf{R}^{N_i}$ and $x_0(t) \in \mathbf{R}^{N_o}$, were observable at equidistant time instants $t_n = n\tau$,

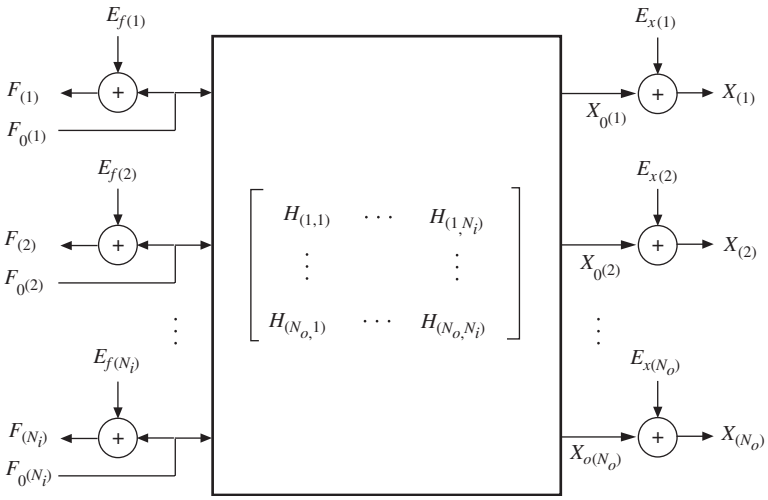

Fig. 1. Multivariable frequency-domain EV setup.

$n = 0, \ldots, N-1$, with τ the sampling period and $T = N\tau$ the observation period, and if the sampled signals could be discrete Fourier transformed without introducing errors (which is the case for periodic signals), then, for all angular frequencies in $\Omega = \{\omega_k = 2\pi k/T : k = 0, \ldots, N/2-1\}$, the following linear mapping would hold exactly

$$X_0(\omega_k) = H(\omega_k)F_0(\omega_k), \tag{2}$$

where $H(\omega_k) \in \mathbf{C}^{N_o \times N_i}$ stands for the *multivariable FRF matrix* at angular frequency ω_k, while $F_0(\omega_k) \in \mathbf{C}^{N_i \times 1}$ and $X_0(\omega_k) \in \mathbf{C}^{N_o \times 1}$ are the corresponding discrete Fourier transforms of the "true" Input/Output signals.

In practice, however, (as illustrated in Fig. 1) errors usually affect the measured Fourier vectors, and consequently, what is observed are not the "true" Input/Output Fourier data, $D_0(\omega_k) = [F_0(\omega_k)^H, X_0(\omega_k)^H]^H$, but $D_0(\omega_k)$ together with some random perturbations, $E_d(\omega_k) = [E_f(\omega_k)^H, E_x(\omega_k)^H]^H$ ($\diamond^H$ stands for the Hermitian transpose operator). The problem, thus, becomes statistical, resulting in random observations, $D(\omega_k) = [F(\omega_k)^H, X(\omega_k)^H]^H$.

Consider now the set $\{(F_m(\omega_k), X_m(\omega_k)) : m = 1, \ldots, M \geqslant N_i\}$ consisting of M observations of the Input/Ouput Fourier vectors at angular frequency ω_k. Using the above notations, the following EV stochastic model relates the M measured observations

$$\left.\begin{aligned} D_m(\omega_k) &= D_{0,m}(\omega_k) + E_{d,m}(\omega_k) \\ [H(\omega_k), -I_{N_o}]D_{0,m}(\omega_k) &= 0 \end{aligned}\right\} \quad m = 1, \ldots, M \geqslant N_i. \tag{3}$$

By grouping the M input and output Fourier vectors into two matrices $\mathscr{F}(\omega_k) = [F_1(\omega_k), \ldots, F_M(\omega_k)] \in \mathbf{C}^{N_i \times M}$ and $\mathscr{X}(\omega_k) = [X_1(\omega_k), \ldots, X_M(\omega_k)] \in \mathbf{C}^{N_o \times M}$, the EV model (3) becomes

$$\begin{cases} \mathscr{D}(\omega_k) = \mathscr{D}_0(\omega_k) + \mathscr{E}_d(\omega_k) \\ [H(\omega_k), -I_{N_o}]\mathscr{D}_0(\omega_k) = 0 \end{cases} \quad \text{with } \mathscr{D}(\omega_k), \mathscr{D}_0(\omega_k), \mathscr{E}_d(\omega_k) \in \mathbf{C}^{(N_i+N_o)\times M} \tag{4}$$

i.e. $\mathscr{D}(\omega_k) = [D_1(\omega_k), D_2(\omega_k), \ldots, D_M(\omega_k)]$, $\mathscr{D}_0(\omega_k) = [D_{0,1}(\omega_k), D_{0,2}(\omega_k), \ldots, D_{0,M}(\omega_k)]$ and $\mathscr{E}_d(\omega_k) = [E_{d,1}(\omega_k), E_{d,2}(\omega_k), \ldots, E_{d,M}(\omega_k)]$.

Note that for a multi-excitation setup, matrix $\mathscr{F}_0(\omega_k)$ of the N_i linear independent stimuli, $\mathscr{F}_0(\omega_k) = [F_{0,1}(\omega_k), \ldots, F_{0,N_i}(\omega_k)] \in \mathbf{C}^{N_i \times N_i}$ has to be of full row-rank, i.e. N_i of the inputs $F_{0,m}(\omega_k) \in \mathbf{C}^{N_i \times 1}$ have to be linearly independent.

An extensive list of statistical publications has been devoted to the closely related topic of EV regression analysis [21–23]. Usually, when an EV model is considered, the covariance matrix of the perturbations, $E_{d,m}(\omega_k)$, is assumed to be a priori known (up to a constant multiplicative factor). An EV model together with

this additional assumption is commonly referred to as the *classical* EV model. Without this additional assumption (or "prejudice"), the problem cannot be solved [17, p. 203].

One way to overcome this problem is to use an instrumental variables approach as presented in Refs. [24,19]. Here, additional information under the form of the ("noise-free") generator signals is used in order to avoid the need for an a priori known noise covariance matrix. The statistical properties for the multivariable formulation of the H_{IV} is discussed in Ref. [19].

In the next section, however, an alternative approach will be proposed based on repeated observations of deterministic signals. This can nowadays easily be realized in practice by applying periodic (broadband) excitations (e.g. multisines) and by measuring, say, $P>1$ periods of the signals. For the case of deterministic excitation, the Instrumental Variables approach then boils down to a special case, i.e. the H_{ML} estimator [19].

3.2. Synchronized deterministic measurements

Nowadays, modal testing equipment has built-in generators permitting the synchronization of the measurements of the applied forces and structures responses automatically. Using a synchronized measurement setup in combination with a deterministic excitation facilitates the observation of the Input/Ouput data for a number of integer periods of the deterministic signal.

Under the condition that repeated observations of the same deterministic excitation signals are available, it is possible to obtain maximum likelihood estimates of the FRFs without requiring any a priori noise information as well as the need for additional instrumental variables.

For a multi-excitation setup, a set of N_i linear independent stimuli, $\mathscr{F}_0(\omega_k)=[F_{0,1}(\omega_k),\ldots,F_{0,N_i}(\omega_k)]\in \mathbf{C}^{N_i\times N_i}$, are required. For the different stimuli, the resulting Input/Ouput data are measured P times (i.e. $M=N_iP$), which leads to the following EV model

$$\left.\begin{aligned} D_p(\omega_k) &= D_{0,p}(\omega_k)+E_{d,p}(\omega_k)\\ [H(\omega_k),-I_{N_o}]D_{0,p}(\omega_k) &= 0 \end{aligned}\right\} \quad p=1,\ldots,P. \tag{5}$$

In Appendix A and Refs. [25,19] it is shown that the maximum likelihood (ML) FRF estimation in this case leads to

$$\hat{H}_{\mathrm{ML}}(\omega_k)=\left(\frac{1}{P}\sum_{p=1}^{P}X_p(\omega_k)\right)\left(\frac{1}{P}\sum_{p=1}^{P}F_p(\omega_k)\right)^{-1}. \tag{6}$$

Note that the covariance matrix of the disturbances is not required anymore to obtain consistent estimates. This estimator belongs to the class of maximum likelihood estimators [21] for which it has been proved that they are consistent and asymptotically efficient. When the errors are not complex normally distributed but have finite moments up to and including order four, then it can be proven that this Gaussian MLE is still consistent but not efficient anymore.

As shown in Appendix B and Ref. [19] the multivariable expression for the estimate of the noise covariance matrix for the MFRFs is given by

$$\mathrm{Cov}(\hat{H}_{\mathrm{ML}}(\omega_k))=\frac{1}{P}\left[\left(\frac{1}{P}\sum_{k=1}^{P}F_k(\omega_k)\right)^{*}\left(\frac{1}{P}\sum_{l=1}^{P}F_l(\omega_k)\right)^{T}\right]^{-1}\otimes C_{\varepsilon}(\omega_k) \tag{7}$$

with

$$C_{\varepsilon}(\omega_k)=\hat{B}(\omega_k)C_{\mathscr{D}}(\omega_k)\hat{B}(\omega_k)^{H},\quad \hat{B}(\omega_k)=\left[\hat{H}_{\mathrm{ML}}(\omega_k),-I_{N_o}\right]. \tag{8}$$

The probability limit (p.lim) for $P\to\infty$ results in the Cramér–Rao lower bound [26], which proves that the H_{ML} is asymptotically efficient. In practice, the data covariance matrix $C_{\mathscr{D}}(\omega_k)$ is determined from repeated measurements under synchronous periodic excitation. The calculation of the power spectra reduces to the calculation of the sample covariance matrix of the synchronized deterministic measurements [26].

In the case of asynchronous periodic measurements, it is possible to use, besides the H_{IV} estimator, FRF estimators based on nonlinear averaging techniques. FRF estimators such as the H_{ari}, H_{har} and the H_{log} are also able to derive the FRF matrix with its covariance matrix under the EV noise model assumptions [27,28]. However, nowadays, modal testing equipment has built-in generators facilitating the automatic synchronization of the measurements. Only in the case that an external generator is used, which cannot be triggered with the data-acquisition system, the input and output signals cannot be synchronized. Recently, an automated spectral analysis of periodic signals was proposed in Ref. [29], for which no synchronization between the generator and the data acquisition is needed. This approach only requires that more than 2 periods of the periodic signal are present in the acquired data.

4. Optimal experiment design

4.1. Crest factor optimization

Consider a flat multisine (i.e., a multisine with equal amplitudes) containing, say, $F = 128$ frequency components. If all phases are put equal to zero, an impact-like signal (see Fig. 2(a)) is obtained with a large crest factor (CF) (CF = 16 for this signal). In order to get measurements with a good signal-to-noise ratio (SNR) the CF should be as small as possible. For comparison, the crest-factor of a sinewave equals $\sqrt{2} \approx 1.414$.

Several algorithms are available to minimize the CF of multisines by specific choices for the phases ϕ_k in Eq. (1). In Fig. 2(b) a so-called Schroeder multisine is given. The Schroeder phases for a flat multisine are given by Ref. [30] $\phi_k = -(\pi k(k-1))/F$. It is possible to further reduce the CF by using optimization-based techniques such as the swapping [31] or the l_∞ algorithm [32]. The l_∞ optimized multisine is given in Fig. 2(c).

For some applications [33,6,7], random multisines (i.e., pseudo-random noise) are preferred, for instance, to average nonlinear effects as explained in Section 5. Note that pseudo-random noise (see Fig. 2(d)) can be considered as being a sub-optimal multisine with equal amplitudes (to approximate white noise) and random phases uniformly distributed in $[0, 2\pi[$.

During modal testing, both input and output signals have to be measured, and thus, all signals should preferably have a good SNR. Assume that, for instance, the Input/Ouput signals are related to each other by a differentiator ($H(s) = \alpha s$). In that case, the resulting output signal for the optimized input of Fig. 2(c) is given in Fig. 3(a). The CF of this signal is not optimal.

Some crest-factor optimization algorithms allow to compress the input as well as the output signals [31,32]. In Figs. 3(b) and (c) the simultaneously optimized Input/Ouput signals are given taking into account the transfer function between input and output. Using these algorithms, it is for instance possible to compress the force signal of a shaker together with the displacement in order not to exceed the stroke limits of the electrodynamic shakers.

4.2. Optimal design of periodic excitations

The quality of the MFRF estimates does not depend on the estimator only, but the excitation plays an important role too. The design of optimal excitations relies on the maximization of the so-called Fisher information matrix [26]. In many systems (e.g. control systems, biological systems) the choice of the excitation is very limited. However, in an important class of problems, only the maximal values of the input and output signals are restricted to maintain the linear behavior of the device under test and/or to avoid overflow of the measurement equipment. This freedom can be used to design *optimal experiments*.

As multi-input modal testing requires uncorrelated inputs, 2 uncorrelated inputs are for instance readily obtained by designing one multisine that only contains odd frequency lines $(f_0, 3f_0, 5f_0, \ldots)$ and another consisting of the even frequencies $(2f_0, 4f_0, 6f_0, \ldots)$ [34,35]. Thus, the use of uncorrelated excitation signals requires the design of as many uncorrelated multisines as there are inputs. In practice, applying uncorrelated excitation signals (multisines, random noise sources, ...) does not necessarily result in uncorrelated input forces. There can be some degree of correlation due to the impedance mismatch between the excitation systems

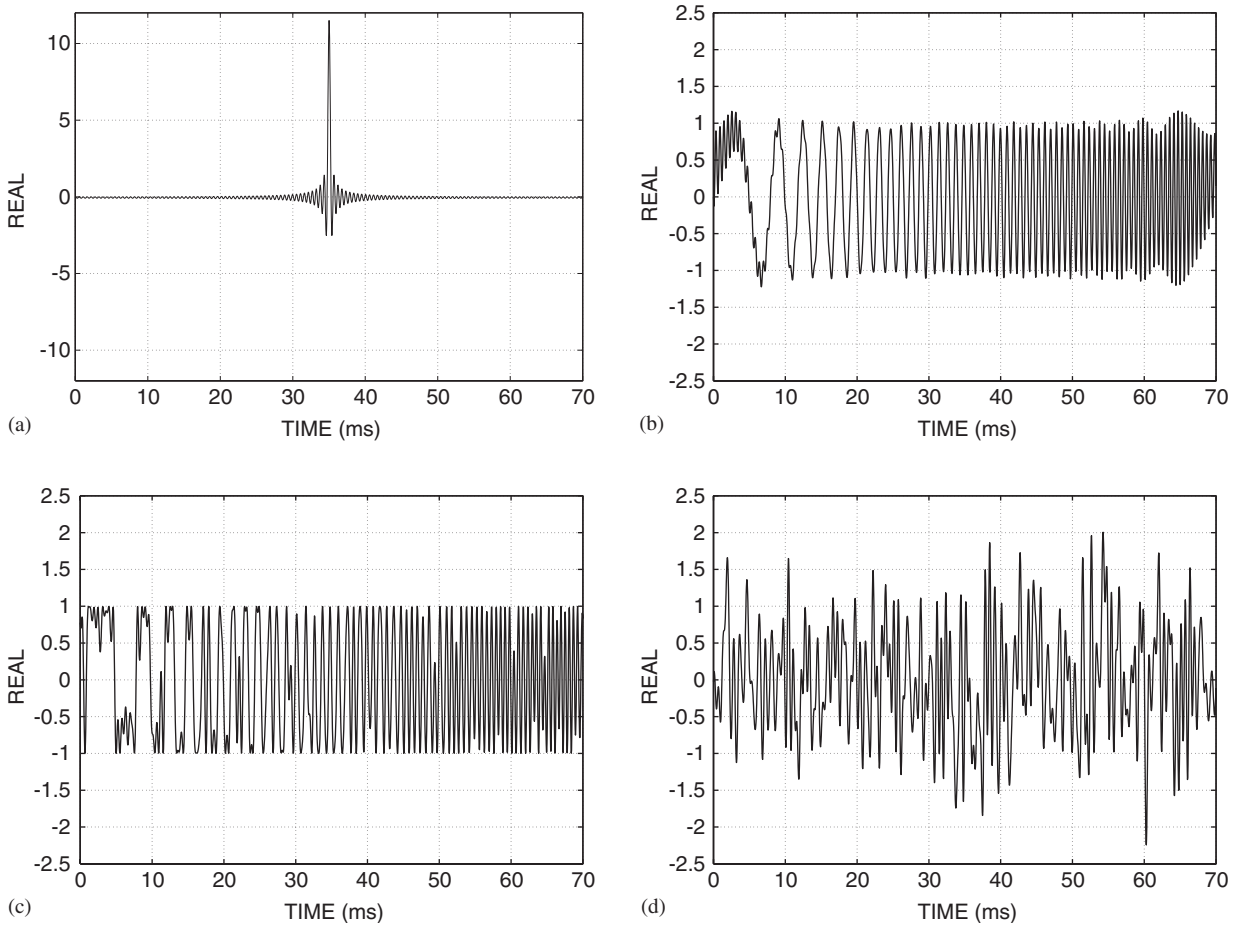

Fig. 2. Comparison of multisines for different phase realizations: (a) zero-phase multisine: CF = 16.00; (b) Schroeder multisine: CF = 1.68; (c) l_∞ multisine: CF = 1.40; and (d) random multisine: CF = 3.07.

and the system under test [36]. Fortunately, the multivariable FRF estimators such as the H_1 or H_{ML} do not require the inputs to be completely uncorrelated.

The design of optimal excitations relies on the minimization of the Cramer–Rao lower bound [26] (or, equivalently, the maximization of the Fisher information matrix, which equals the inverse of the Cramer–Rao matrix). It can be shown that the Cramer–Rao lower bound of the MFRF estimate is given by

$$C_{\mathrm{CR}}(\mathrm{vec}(H(\omega_k))) = \frac{1}{P}(\mathscr{F}_0(\omega_k)^T \mathscr{F}_0(\omega_k)^*)^{-1} \otimes C_{B_D}(\omega_k), \tag{9}$$

where $\mathrm{vec}(H(\omega_k)) = (H_{11}, \ldots, H_{N_o 1}, H_{12}, \ldots, H_{N_o N_i})^T$, $C_{B_D}(\omega_k) = BC_{\mathscr{D}}B^H$ and $B(\omega_k) = [H(\omega_k), -I_{N_o}]$. This result is a generalization of Theorem 8.2.5 in Ref. [15] where only output disturbances are considered. The Cramer–Rao matrix is a lower bound for the covariance matrix $\mathrm{Cov}(\hat{H}_{\mathrm{ML}}(\omega_k))$ of the maximum likelihood estimate $\hat{H}_{\mathrm{ML}}(\omega_k)$. Thus, to decrease this lower bound, one has to minimize $\det(C_{\mathrm{CR}}(\mathrm{vec}(H(\omega_k))))$ (i.e., so-called D-optimal design [37]), which equals

$$\det(C_{\mathrm{CR}}(\mathrm{vec}(H(\omega_k)))) = \frac{1}{P^{N_i N_o}} \frac{\det(C_{B_D}(\omega_k))^{N_i}}{\det(\mathscr{F}_0(\omega_k)^T \mathscr{F}_0(\omega_k)^*)^{N_o}}. \tag{10}$$

As a result, the optimal input design is the one that maximizes $|\det(\mathscr{F}_0(\omega_k))|$.

Assume that we have designed, for a given frequency band, a multisine with optimized crest-factor. Its Fourier coefficient at angular frequency ω_k will be denoted by $S(\omega_k)$. Applying this signal (with normalized

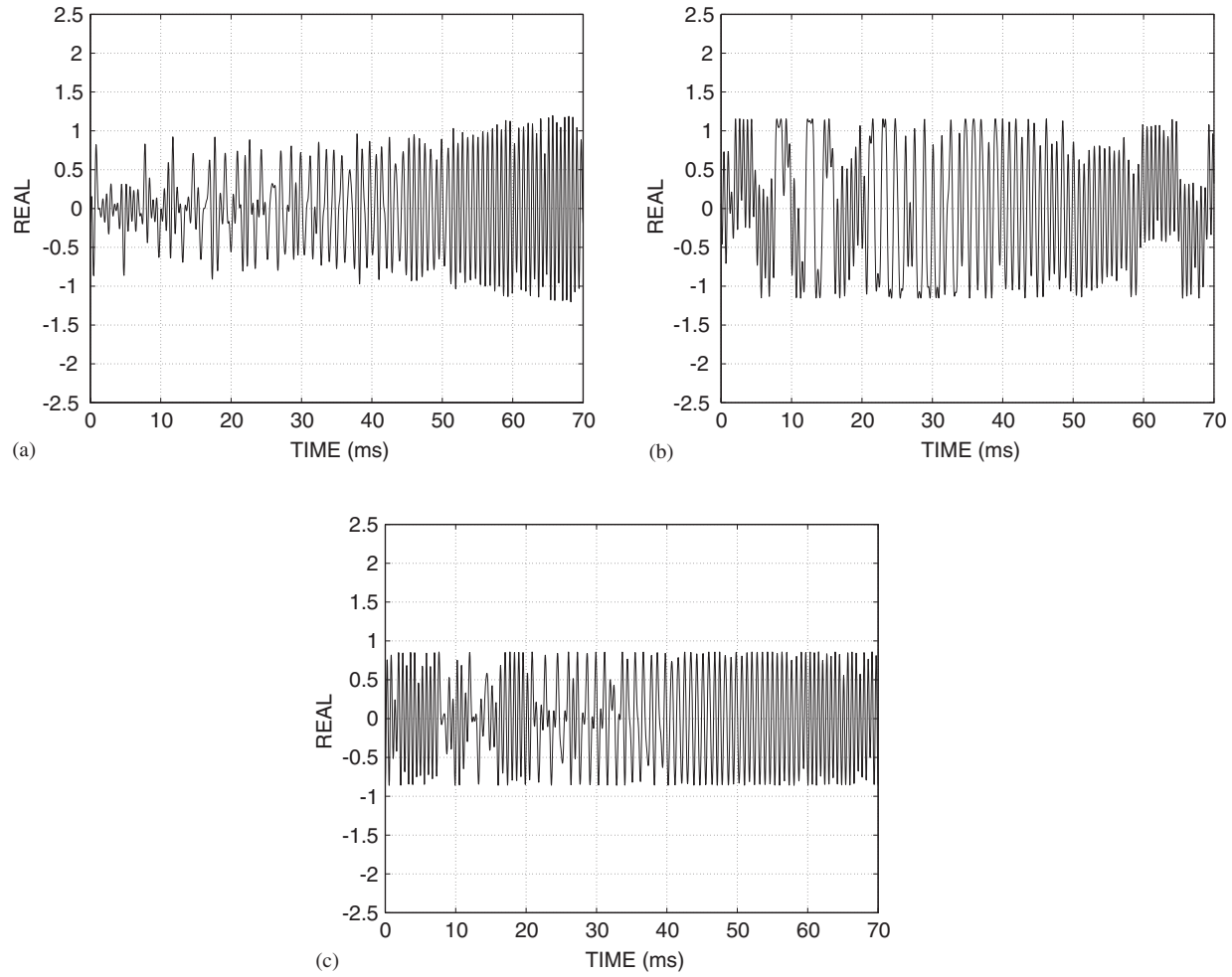

Fig. 3. Input/Ouput CF optimization: (a) Output signal: CF = 2.25; (b) Optimized input: CF = 1.61; and (c) Optimized output: CF = 1.61.

peak value) to the different inputs, taking into account the maximum allowed peak values R_i, $i = 1, \ldots, N_i$, results for observation p in the input vector

$$F_{0,p}(\omega_k) = (R_1 S(\omega_k) Q_{1,p}, R_2 S(\omega_k) Q_{2,p}, \ldots, R_{N_i} S(\omega_k) Q_{N_i,p})^T. \tag{11}$$

The question that has to be addressed now is how to choose the matrix $Q \in [-1, 1]^{N_i \times N_i}$ such that $|\det(\mathscr{F}_0(\omega_k))|$ attains its extremum. The answer follows from Lemma 2 in Appendix C showing that the extremum is obtained when Q is a Hadamard matrix [4]. For instance, for $N_i = 2$, $Q = \begin{bmatrix} 1 & -1 \\ 1 & 1 \end{bmatrix}$ is optimal, and for $N_i = 3$, $Q = \begin{bmatrix} 1 & -1 & -1 \\ 1 & 1 & -1 \\ 1 & 1 & 1 \end{bmatrix}$.

5. Detection and characterization of nonlinear distortions

The most simple method for the detection of nonlinear distortions is the sine test, characterizing nonlinear behavior by checking on the generation of higher harmonics. However, this method is very slow and it is unacceptable that most of the available measurement time should be spent on the detection of nonlinear distortions at the cost of reduced FRF quality. Another approach, commonly-used in modal testing, is based

on random noise measurements at increasing excitation levels and comparing the FRFs that should be amplitude independent in the linear range of the system. This method is also less appealing since two separate measurements are needed and a possible nonlinear load behavior of the generator can occur due the input impedance of the tested system. Another often-used test is the coherence check, which however does not allow one distinguish between noise disturbances, leakage errors and nonlinear distortions.

Using random noise signals, small nonlinear distortions can still be reduced by sufficient averaging. This results in the so-called "best linear approximation" for the system, although it introduces the important disadvantages of leakage and transient effects. As a result, the class of suitable excitation signals is already restricted to broadband random multisines. Depending on the measurement procedure and specific choice of the amplitude spectrum two approaches, that allow the detection, qualification and quantification of nonlinear distortions during FRF measurements, are now discussed.

5.1. Approach 1: Use of pseudorandom excitation

This approach is based on using random multisine or so-called pseudorandom excitations in a special periodic measurement sequence. A pseudorandom signal is typically constructed with harmonic components of equal amplitudes and random phases uniformly distributed in $[0, 2\pi[$, every line containing equal energy in the frequency band considered.

This approach allows one to measure in the same experiment the nonlinear and disturbing noise levels. This is done by analyzing the variations over consecutively measured periods, and the variations over different realizations of the input signal as is now briefly discussed (cf. Refs. [6,7,10,9] for details). Consider again the multivariable "errors-in-variables" setup in Section 3.1 and Fig. 1. Using the FFT, the measured input and output signals for each individual period m are denoted by $\mathscr{F}_{[r,m]}(\omega_k)$, $\mathscr{X}_{[r,m]}(\omega_k)$, with $r = 1, \ldots, R$ indicating the different realizations for the pseudorandom input and $m = 1, \ldots, M$ ($M = N_i P$) indicating P measured periods of the periodic repetition of each realization according e.g. a N_i multi-input scheme maximizing the Fisher information matrix as explained in Section 4.2.

Assuming for conciseness that there is no noise on the input, both input and output relations are then given as

$$\mathscr{F}_{[r,m]}(\omega_k) = \mathscr{F}_{[r]}(\omega_k), \tag{12}$$

$$\mathscr{X}_{[r,m]}(\omega_k) = H_R(\omega_k)\mathscr{F}_{[r]}(\omega_k) + T_{[r,m]}(\omega_k) + \mathscr{S}_{\mathscr{X}_{[r]}}(\omega_k) + \mathscr{N}_{\mathscr{X}_{[r,m]}}(\omega_k) \tag{13}$$

with $T_{[r,m]}(\omega_k)$ a transient term, $\mathscr{S}_{\mathscr{X}_{[r]}}(\omega_k)$ the stochastic nonlinearities and $\mathscr{N}_{\mathscr{X}_{[r,m]}}(\omega_k)$ the disturbing noise. As can be seen from the output relation, the following patterns are derived:

- For a given realization r the variations from one period to another are only due to the disturbing noise and the vanishing transient effects. Thus averaging over consecutive periods m will only reduce the effects of the disturbing noise, while the nonlinear distortions not depending on m do not disappear if more periods are averaged (increasing M). As a result, applying a given realization of a pseudo random multisine for a sufficient number of consecutive periods yields the combined stochastic error due to both the disturbing noise and nonlinear distortions.
- Applying different realizations r for the pseudorandom multisine, the variations from one period to another are now due to the disturbing noise, the vanishing transient effects and the nonlinear distortions. Hence, in order to reduce the effects of the nonlinear distortions, averaging over different realizations should be increased (by increasing R). As a result, applying sufficient different pseudorandom realizations yields the stochastic error due solely to the disturbing noise.

Given the random character of the applied multisine signal, this approach combines in one experiment the measurement of the "best linear approximation" of the MFRFs together with the detection of the error levels due to disturbing noise and nonlinear distortions. The generally large number of averages can be reduced by the use of CF optimized pseudorandom signal realizations [8].

5.2. Approach 2: Use of odd–odd multisine excitation

The basic idea of this approach relies on exciting the system with an odd–odd multisine, where only the frequencies $4k+1,\ k=0,1,2,\ldots,k_{\max}$ in Eq. (1) have amplitudes different from zero. The output spectrum $X(\omega_k)$, calculated using an FFT and rectangular window again forms the basis for the detection of nonlinear distortions. As discussed in Ref. [8], it holds that even nonlinearities excite only the even harmonics at the output $(2k, k=1,2,\ldots)$, while the odd nonlinearities appear only at the odd harmonics $(2k+1, k=1,2,\ldots)$. As a result of the specific choice of excitation signal, the output spectrum contains the following information for $k=0,1,2,\ldots,k_{\max}$:

- At lines $4k+1$: the output consisting of the linear contribution and odd nonlinear distortions.
- At lines $4k+2$: only the even nonlinear distortions.
- At lines $4k+3$: only the odd nonlinear distortions.

This enables both the detection and characterization of the system's nonlinear behavior. If at least $P \geqslant 2$ successive periods are measured in one block, it is still possible to make the same conclusions at respectively lines $P(4k+1)$, $P(4k+2)$ and $P(4k+3)$. In addition, it is also possible to derive the noise level (having a nonperiodic behavior) at the lines that are not a multiple of P since these cannot be excited by a signal with M periods in a single block (window).

In the end, the engineer derives from one single experiment the broadband MFRF measurement and the detection, qualification and rough quantification of the nonlinear distortions, together with a noise analysis. The price for this is a loss in frequency resolution caused by the nonexcited lines or an increased measurement time (factor 4) by increasing the number of frequency lines to maintain the same resolution. The "best linear approximation" for the studied system is obtained by applying odd–odd multisines with optimized crest factor optionally combined with averaging over different realizations of the (random) odd–odd multisine at the cost of an increased measurement time.

Remark. In practice, some additional problems can occur during modal testing using this approach. A nonlinear interaction between the generator and the studied system can generate unwanted excitations at the detection frequencies or create additional undesired harmonic components once the system becomes nonlinearly distorted. Hence, it is no longer clear what part of the output should be assigned to the system behavior and what part is due to the nonlinear interaction distortions. In that case, the output can be compensated through a first-order correction $\tilde{X}(\omega_k) = X(\omega_k) - \tilde{H}(\omega_k) \cdot F(\omega_k)$, where $\tilde{H}(\omega_k)$ is obtained by a linear interpolation between the FRF measurements at the excited frequencies.

6. Experimental results for body-in-white structure

The applicability of the presented methods was studied for the case of a typical modal test of a so-called "body-in-white" structure as shown in Fig. 4. The car body was suspended by means of steel cables connected to the car body through 4 sets of 3 springs connected at the front and back part of the body. Multiple-input testing was realized using 2 Bruël & Kjær shakers in the front part where the applied loading was measured using PCB force sensors. Multiple responses were measured using PCB accelerometers and the results presented for this specific study used 2 of the observed responses (1 sensor at the coupling of multiple parts by means of welding and screw joints (see Fig. 4), the other on a side panel). The measurements were controlled using MATLAB software in combination with a National Instruments data-acquisition board (with synchronized 2 generators and 16 channels). Reason for this choice is the fact that until today commercially available measurement systems still do not provide sufficient freedom in the application of "exotic" excitation signals such as the odd–odd multisines.

The following issues were considered during the performed modal testing experiments:

- Three types of different excitation signals were considered during the experiments: random noise, pseudo random (random multisine) and l_∞ optimized odd–odd multisine.

Fig. 4. Modal test setup for car body: (left) view on suspended car body, (middle) shakers applying dynamic loading to the car and (right) response sensor nearby a welded/screwed joint.

Table 1
Summary of excitation signals and data-acquisition parameters for three different experiments

Experiment	1	2	3
Signal type	Random noise	Pseudo random	l_∞ odd–odd
Crest factor	3.156	2.391	1.084
# Consec. blocks P ($M = N_i.P$)	1	10	10
# Realizations R	10	10	1
Source level (low) (Vrms)	1.5	2.0	1.5
Source level (high) (Vrms)	4.0	4.5	3.5

- Multiple input testing required the generation of uncorrelated inputs. As discussed in Section 4.2, this can be realized by generating a single multisine (e.g. pseudo random or odd–odd) and applying, in this practical case, this signal through two ($N_i = 2$) subsequent load realizations according to the optimal Hadamard $\begin{bmatrix} 1 & -1 \\ 1 & 1 \end{bmatrix}$ matrix realization. For the random noise excitation, two different random noise realizations were applied as is classically done in modal testing practice.
- A CF optimization (cf. Section 4.1) was applied for the odd–odd multisine excitation since only one realization was used during the experiment. In order to find the "best linear approximation" of the measured FRFs for the studied car body it is advised to use a CF optimization when applying odd–odd excitation. Notice that a CF optimization could also be applied for the pseudo random excitation. However, since this signal was applied during a sufficient number of consecutive periods and for different realizations, the averaging process generally yields a "best-practice best linear approximation" without the need for CF optimization (which also would increase the measurement time since the iterative l_∞ optimization algorithm would have to be executed for each realization).
- Two different estimators are considered during the nonparametric processing of the acquired data in order to estimate the multivariable FRFs and their corresponding noise covariance matrix as discussed in Section 3.2. For the random noise experiment, the classical H_1 is used, while the EV approach could be applied for the multisine (pseudo and odd–odd) cases.
- Three different experiments were performed in this study as summarized in Table 1. Both approaches for the detection and characterization of nonlinear distortions during the FRF measurements, as presented in Section 5, were applied for, respectively, the pseudo random and odd–odd multisine excitation. It should be noticed that the total number of averages available for the nonparametric processing and assessment of nonlinear distortions was 10 times larger for the experiment using the pseudo random excitation. This because 12 consecutive periods (2 periods waiting for vanishing transient effects) were acquired for each of the 10 pseudo random realizations. On the contrary, 12 consecutive periods were acquired for just 1

odd–odd multisine realization that has in its turn a frequency resolution that is 4 times larger than the pseudo random excitation in order to introduce detection lines in the excitation spectrum.
- For comparison reasons the measurement channel settings (channel ranges, anti-aliasing filters, ...) were kept the same throughout this study.

Remark. Consider a multisine and random noise excitation with the same number of spectral lines in the observed Fourier data. Since a multisine signal typically has a constant amplitude spectrum, every spectral line receives enough energy during a single record resulting in a good SNR for each spectral line. This is certainly not the case for a random noise excitation so that the number of required records for random noise excitation is always larger in order to obtain the same data quality compared to a multisine. As a result, a given data quality is achieved with less measurement time in the case of a multisine. When using the specially designed odd–odd multisine, the number of spectral lines is increased with a factor 4 in order to introduce the detection lines while keeping the same frequency resolution for the excited spectrum. As a result, in one record, the odd–odd multisine permits acquiring, besides system information, also information on the measurement setup (noise) and possible nonlinear behavior of the studied system, at the cost of an increased measurement time for a single record. However, with respect to achieving a certain data quality (in terms of SNR) in comparison to random noise, it still applies that the same quality is achieved with much less observed records in the case of the odd–odd multisine.

Fig. 5 shows the error levels (standard deviations) for the FRF estimates derived from the noise covariance matrices, for the three different types of excitations. These matrices are computed during the nonparametric

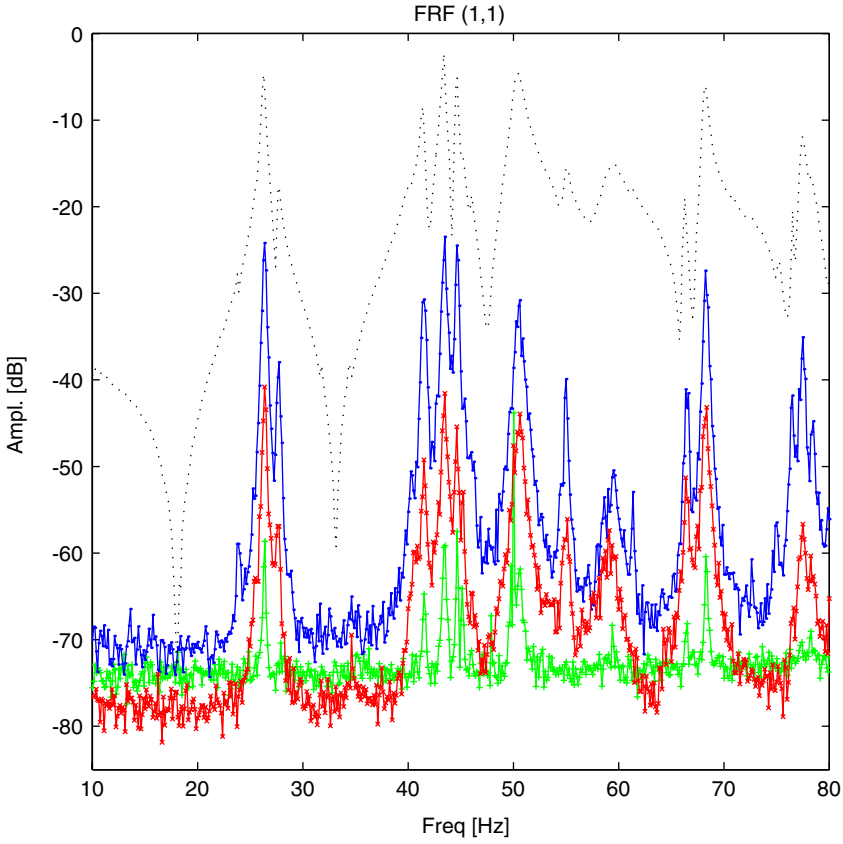

Fig. 5. Stochastic error (variance) on the FRF for different excitation signals: (−) FRF(1, 1), (−•) random noise, (−×) random multisine, (−+) odd–odd multisine. The FRF and the variances on the FRF are given in dB scale (i.e. $20\log_{10}(|H|)$ with H the FRF).

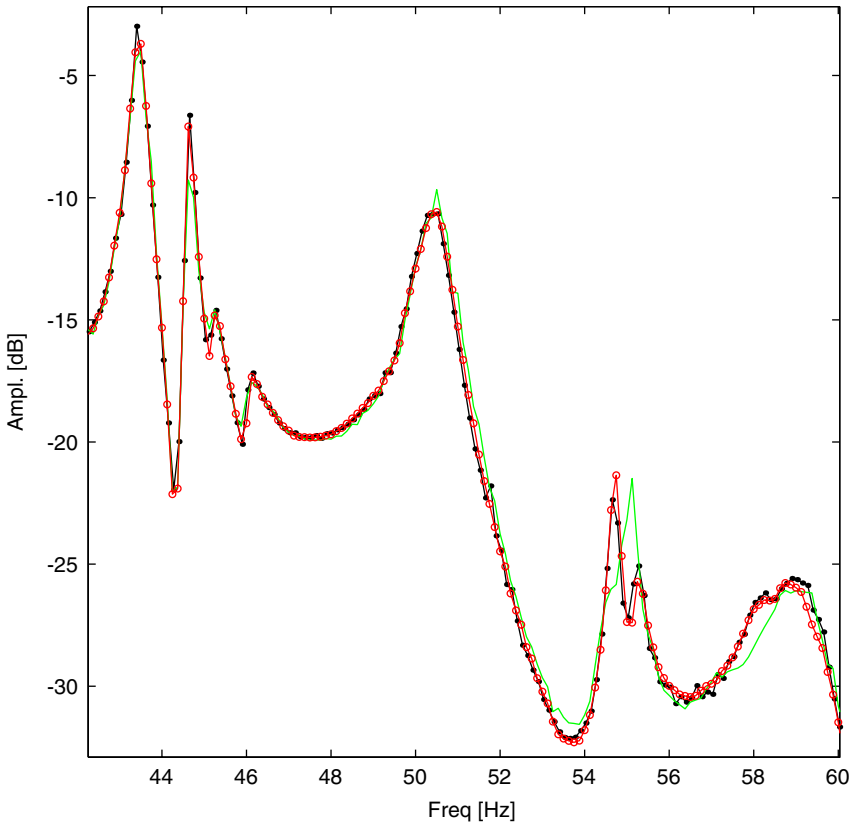

Fig. 6. Comparison of H_1 and H_{ML} FRF (1, 2) estimates (zoom on band in Fig. 5): (−) H_1 random noise, (−+) H_{ML} random multisine, (−•) H_{ML} odd–odd multisine. The FRFs are given in dB scale (i.e. $20\log_{10}(|H|)$ with H the FRF).

averaging process and multivariable expressions for the H_1 and H_{ML} are given in Ref. [19] and Section 3. As can be seen, the stochastic errors on the FRFs are smallest for the experiment using an l_∞ optimized odd–odd multisine combined with the H_{ML} FRF estimator. The largest errors are related to the random noise excitation mainly due to lower SNR for the measured signals within a single observation window (the number of averages is the same as for odd–odd experiment), while a lower crest factor and a larger number of averages (compared to the random noise case) reduces the stochastic errors on the FRF estimates obtained by the pseudo random experiment.

Although the noise levels on the measured force signals were small in the data-acquisition setup, a gain in accuracy is still obtained from taking also the input noise into account during nonparametric processing based on an EV stochastic framework. This can also be observed in Fig. 6, where especially in the resonances (peaks) the differences (typically 2 to 5 dB for this case) between the H_1 (random noise) and the H_{ML} (pseudo/odd–odd) are due to systematic (bias) errors in the H_1 FRF estimates [24,19].

The effects of an increasing excitation amplitude on the FRF estimates can be observed in Fig. 7 for the experiment using random noise excitation combined with the H_1 estimator. It is seen that the resonance peaks shift to lower frequencies and become broader with lower amplitude due to an increasing effect of nonlinear distortions during the FRF measurements. Physically, this behavior can be related to the nonlinear characteristics of the car body's material properties, where the damping characteristics change and the Young's modulus becomes smaller at larger vibration amplitudes and hence larger displacements result. Since the Young's modulus is also proportional to the material stiffness, the resonance frequencies tend to decrease (in this case by typically up to 1 Hz with the frequency resolution $\Delta f = 0.0125$).

Fig. 8 illustrates the detection of nonlinear distortions using *approach* 1 with a pseudorandom excitation as discussed in Section 5.1. Based on the averaging-based nonparametric analysis of the response spectra (−) for

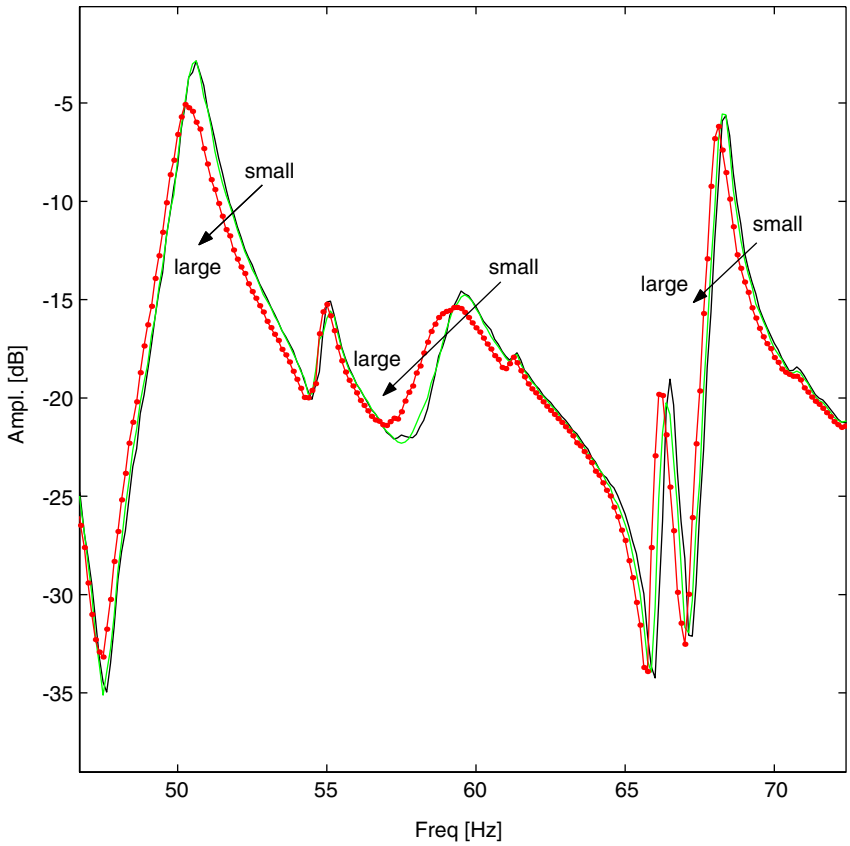

Fig. 7. Effect of increasing excitation amplitude on FRF for random noise. The FRFs are given in dB scale (i.e. $20\log_{10}(|H|)$ with H the FRF).

the different multi-input realizations ("even" stands for $\{^{1}_{1}\}$ and "odd" for $\{^{1}_{-1}\}$) and different pseudorandom realizations, the engineer gets a better insight in the errors on the FRF estimates, since a separation between the disturbing noise level ($-\bullet$) and the level of errors due to both the disturbing noise and nonlinear distortions ($-\times$) becomes possible. The difference between low and high excitation levels (cf. Table 1) is clearly observed. For a low amplitude excitation, both error contributions are of the same level, while at a high amplitude the error level for the combined noise and nonlinear distortions contributions is clearly higher, typically by 10–25 dB, than the disturbing noise level. Notice also that this difference varies with the Input/Ouput locations, which is related to the car body's construction in terms of welding and screwing joints as well as the material itself (i.e. high vibration amplitudes in the panel parts of the body).

More detailed information for the detection, qualification and a rough quantification is derived by *approach* 2 by the use of odd–odd multisine excitation. As explained in Section 5.2, the nonparametric analysis of the response spectrum (optionally by averaging consecutive periods) can be done by separating the spectral energy present at the excited and non excited even/odd frequency lines. This results in Fig. 9 with the response spectrum ($-$), disturbing noise ($-\bullet$), even nonlinear distortions ($-\times$) and odd nonlinear distortions ($-+$). Again, it can be seen that for a low level of excitation the different error levels coincide, which indicates that the nonlinear distortions are of the same level as the stochastic error due to the disturbing noise (SNR for the response signals is 40–60 dB). Increasing the excitation amplitude clearly results in an increasing effect of nonlinear distortions. The levels for the even and odd nonlinear distortions are now about 20–30 dB higher than the disturbing noise, clearly indicating the dominance of nonlinear distortions in the overall error on the observed responses. Moreover, more detailed information about the character of the nonlinearities as a function of the frequency is derived by *approach* 2. It is noticed that the portion of even nonlinear distortions is still about 8–12 dB higher than the odd nonlinear contribution, and so for the studied body-in-white structure,

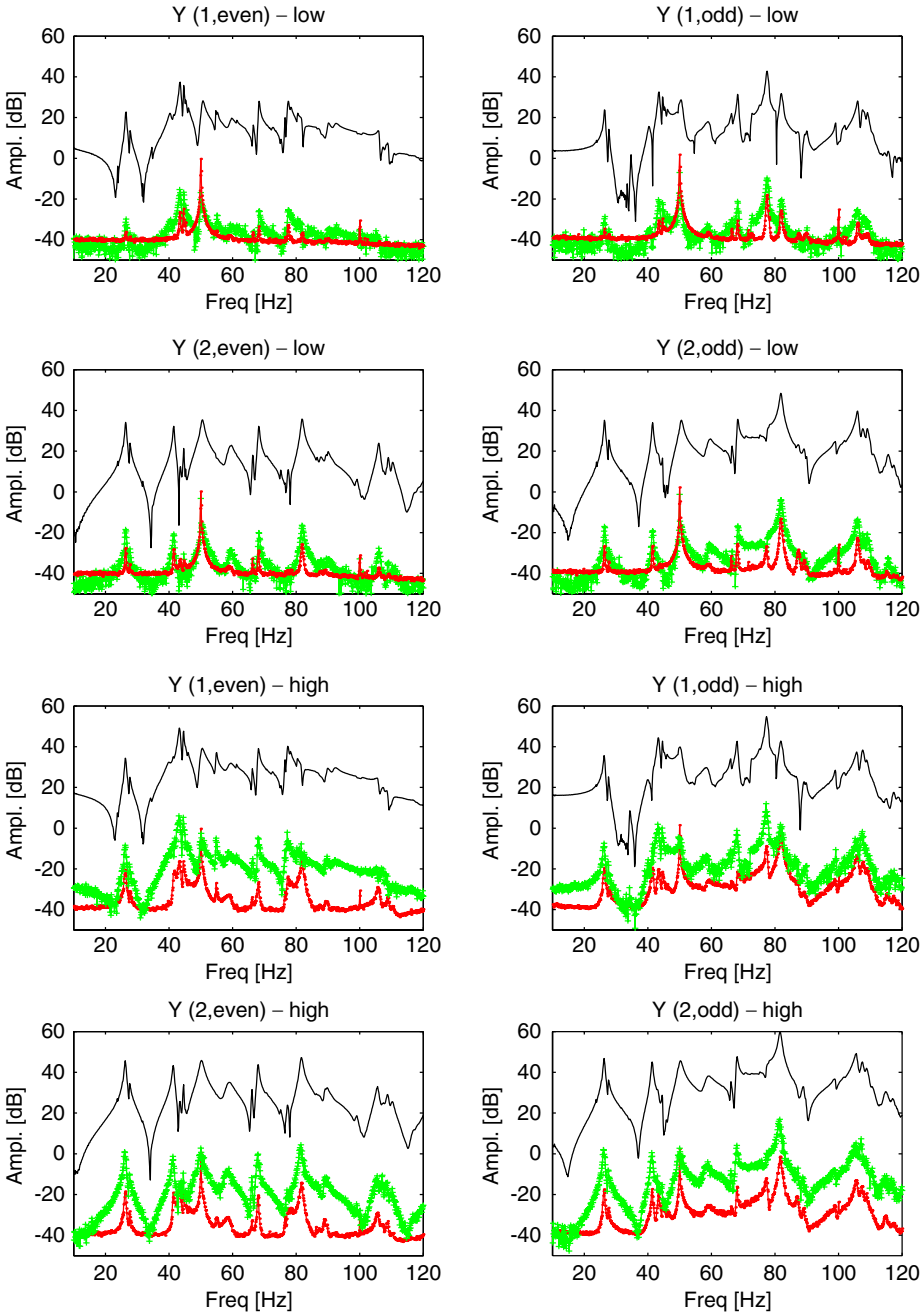

Fig. 8. Detection of nonlinear distortions at output using *approach* 1 with a pseudo random excitation: low-level (top) and high-level (bottom)—(−) measured response, (−•) disturbing noise, (−×) disturbing noise + nonlinear distortions. The response spectra are given in dB scale (i.e. $20\log_{10}(|Y|)$ with Y the response spectrum).

the even nonlinear distortions seem to be most dominant. Another important observation is the fact that increasing the amplitude during modal testing is generally perceived as beneficial for the SNR of the measured signals, which is only correct around the linear working point of the considered structure. However, as can be seen from the results acquired on the car body, for both a low or high level of excitation the disturbing noise level remains the same, while only the nonlinear contributions are enforced during testing at higher

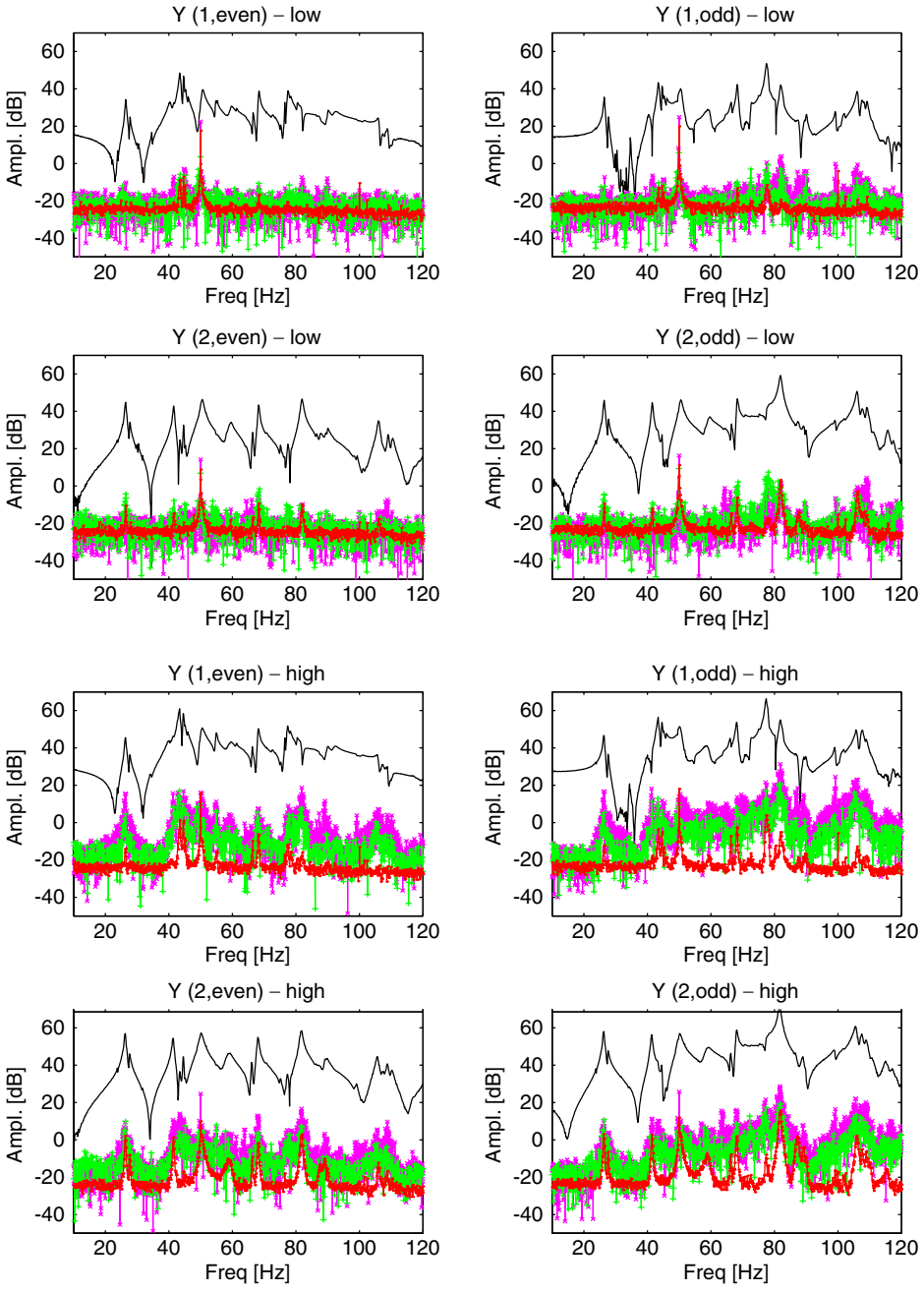

Fig. 9. Detection of nonlinear distortions at output using *approach* 2 with an l_∞ optimized odd–odd excitation: low-level (top) and high-level (bottom)—(−) measured response, (−•) disturbing noise, (−×) even nonlinear distortions and (−+) odd nonlinear distortions. The response spectra are given in dB scale (i.e. $20\log_{10}(|Y|)$ with Y the response spectrum).

amplitudes. It can be concluded that both approaches presented in Section 5 provide powerful tools for the engineer in order to assess the presence and character of nonlinear distortions during FRF measurements and more general during modal testing. Performing the correction on the output spectrum for possible extraneous nonlinear distortions, as discussed in Section 5.2, yields the same results. In this case, the nonlinear distorting effects of the shakers were kept very small by the use of high quality shaker-amplifier systems in their optimal working point (range).

7. Conclusions

In this paper new developments for modal testing have been discussed. First, attention has been paid to the maximum likelihood estimation of multivariable FRFs and their noise covariance matrix from multisine measurements when using a synchronized setup. It is shown that this estimator outperforms the classically-used FRF estimators. Next, the optimization of the CF of multisines as well as the application of multisines for multi-input excitation have been included in a modal testing procedure. It is shown that simply by the use of one single multisine realization, multi-input testing is possible based on an excitation scheme that maximizes the so-called Fisher information matrix. Moreover, with the application of multisine excitations, it becomes possible to measure the FRFs simultaneously with detection, qualification and quantification of the nonlinear distortions during testing. In cases where nonlinear distortions are not avoidable, random multisine testing still allows the measurement of the "best linear approximation" of the studied system. Finally, the benefits and at the same time ease-of-application of the different tools to be included in a typical multivariable modal testing procedure have been illustrated by means of experimental results for an application in the field of automotive engineering vibration analysis.

Acknowledgements

The financial support of the Institute for the Promotion of Innovation by Science and Technology in Flanders (IWT), the Concerted Research Action "OPTIMech" of the Flemish Community and the Research Council (OZR) of the Vrije Universiteit Brussel (VUB) are gratefully acknowledged.

Appendix A. Maximum likelihood estimation of MFRFs

Recalling the EV model (5) where the inputs $F_{0,p} = F_{0,p}(\omega_k)$ (ω_k is omitted for simplifying notations) are considered deterministic. It will be assumed that the random vectors $\{E_{d,p} : p = 1, \ldots, P\}$ are complex normally distributed with

$$\mathrm{Cov}(E_{d,k}, E_{d,l}) = C_{\mathscr{D}}\delta_{kl} \tag{14}$$

and $C_{\mathscr{D}} \in \mathbf{C}^{(N_o+N_i)\times(N_o+N_i)}$ an a priori known Hermitian-symmetric covariance matrix. Notice that C_D accounts for possible correlations among the Input/Ouput Fourier coefficients. For a wide class of probability density functions of the time-domain noise, the Fourier coefficients are *asymptotically* (as the number of time samples $N \to \infty$) complex normally distributed and independent over the frequencies [15]. This motivates the use of a complex Gaussian *probability density function* (PDF) to construct the MLE. The (asymptotical) independence over the frequencies allows us to write the ML equations for a single frequency.

This results in the following (negative) log-likelihood function

$$\ell(\hat{H}, \hat{\mathscr{F}}) = \sum_{p=1}^{P} \mathrm{tr}\left(C_{\mathscr{D}}^{-1} \left[D_p - \begin{Bmatrix} I_{N_i} \\ \hat{H} \end{Bmatrix} \hat{\mathscr{F}} \right] \left[D_p - \begin{Bmatrix} I_{N_i} \\ \hat{H} \end{Bmatrix} \hat{\mathscr{F}} \right]^H \right). \tag{15}$$

The matrices $\hat{H}$ and $\hat{\mathscr{F}} = [\hat{F}_1, \ldots, \hat{F}_P]$ are the independent variables, while $\mathscr{D} = [D_1, \ldots, D_P]$ represents the measurements. The values of the independent variables minimizing the cost function (15) are the MLEs $(\hat{H}_{\mathrm{ML}}, \hat{\mathscr{F}}_{\mathrm{ML}})$ of the true $(H, \mathscr{F}_0)$ while the MLE of the dependent variable $\mathscr{X}_0$ is given by

$$\hat{\mathscr{X}}_{\mathrm{ML}} = \hat{H}_{\mathrm{ML}}\hat{\mathscr{F}}_{\mathrm{ML}}. \tag{16}$$

Thereto the method of the Lagrangian multipliers is applied to Eq. (15), resulting in

$$\ell(\hat{H}, \hat{\mathscr{D}}, \hat{L}) = \sum_{p=1}^{P} \mathrm{tr}(C_{\mathscr{D}}^{-1}[D_p - \hat{\mathscr{D}}][D_p - \hat{\mathscr{D}}]^H) + \mathrm{Re}(\mathrm{tr}(\hat{L}^H\hat{B}\hat{\mathscr{D}})), \tag{17}$$

where $\hat{\mathscr{D}} \in \mathbf{C}^{(N_o+N_i)\times N_i}$, $\hat{B} = [\hat{H}, -I_{N_o}] \in \mathbf{C}^{N_o\times(N_o+N_i)}$ and where $\hat{L}$ is a Lagrangian multiplier matrix for the constraint $\hat{B}\hat{\mathscr{D}} = 0$ (use of the real part of the trace of $\hat{L}^H\hat{B}\hat{\mathscr{D}}$ is just a convenient way of summing $\mathrm{Re}(\hat{L}_{jk})\,\mathrm{Re}(\sum_l \hat{B}_{jl}\hat{\mathscr{D}}_{lk})$ and $\mathrm{Im}(\hat{L}_{jk})\,\mathrm{Im}(\sum_l \hat{B}_{jl}\hat{\mathscr{D}}_{lk})$ over all j, k). In its extremum, $\ell(\hat{H}, \hat{\mathscr{D}}, \hat{L})$ must be stationary

with respect to $\hat{H}$, $\hat{\mathscr{D}}$ and $\hat{L}$. Setting $\partial\ell/\partial\,\mathrm{Re}(\hat{\mathscr{D}}) + \sqrt{-1}\partial\ell/\partial\,\mathrm{Im}(\hat{\mathscr{D}})$ equal to zero gives (notice that ℓ is not an analytic function, thus, $\partial\ell/\partial\hat{\mathscr{D}}$ does not exist).

$$-2C_{\mathscr{D}}^{-1}\left(\sum_{p=1}^{P} D_p - P\hat{\mathscr{D}}\right) + \hat{B}^H\hat{L} = 0. \tag{18}$$

Similarly, the derivative with respect to $\mathrm{Re}(\hat{H})$ and $\mathrm{Im}(\hat{H})$, respectively $\mathrm{Re}(\hat{L})$ and $\mathrm{Im}(\hat{L})$ give

$$\hat{L}\hat{\mathscr{F}}^H = 0, \tag{19}$$

$$\hat{B}\hat{\mathscr{D}} = 0. \tag{20}$$

As $\hat{\mathscr{F}} \in \mathbf{C}^{N_i\times N_i}$ is a regular matrix by assumption, (19) can only be satisfied when $\hat{L} \in \mathbf{C}^{(N_o+N_i)\times N_i}$ equals zero. Consequently, Eq. (18) reduces to

$$\hat{\mathscr{D}} = \frac{1}{P}\sum_{p=1}^{P} D_p \tag{21}$$

and, by way of Eq. (20), the transfer matrix estimate $\hat{H}_{\mathrm{ML}}$ becomes

$$\hat{H}_{\mathrm{ML}} = \left(\frac{1}{P}\sum_{p=1}^{P} X_p\right)\left(\frac{1}{P}\sum_{p=1}^{P} F_p\right)^{-1}. \tag{22}$$

Note that a priori knowledge of $C_{\mathscr{D}}$ is not required any more to obtain the ML estimate of H.

Appendix B. Covariance matrix of the MFRF ML estimates

Defining $\hat{\mathscr{X}} = \frac{1}{P}\sum_{k=1}^{P} X_k$ and $\hat{\mathscr{F}} = \frac{1}{P}\sum_{l=1}^{P} \mathscr{F}_l$, Eq. (6) can also be written as

$$\hat{H}_{\mathrm{ML}} = \hat{\mathscr{X}}\hat{\mathscr{F}}^{-1}. \tag{23}$$

Starting from a sensitivity analysis, an expression for the covariance matrix of the $\hat{H}_{\mathrm{ML}}$ FRF estimates can be found

$$\delta(\hat{H}_{\mathrm{ML}}) = \delta(\hat{\mathscr{X}})\hat{\mathscr{F}}^{-1} + \hat{\mathscr{X}}\delta(\hat{\mathscr{F}}^{-1}) \tag{24}$$

with $\delta(\hat{\mathscr{F}}^{-1}) = \hat{\mathscr{F}}^{-1}\delta(\hat{\mathscr{F}})\hat{\mathscr{F}}^{-1}$. Using the Vector vec and Kronecker $\otimes$ operators, this can also be written as

$$\mathrm{vec}(\delta\hat{H}_{\mathrm{ML}}) = (\hat{\mathscr{F}}^{-T}\otimes I_{N_o})\,\mathrm{vec}(\delta\hat{\mathscr{X}}) - (\hat{\mathscr{F}}^{-T}\otimes\hat{\mathscr{X}}\hat{\mathscr{F}}^{-1})\,\mathrm{vec}(\delta\hat{\mathscr{F}}) \tag{25}$$

the covariance matrix of the $\hat{H}_{\mathrm{ML}}$ FRF matrix is then given by

$$\begin{aligned}\mathrm{Cov}(\hat{H}_{\mathrm{ML}}) &= \mathscr{E}\{\mathrm{vec}(\delta\hat{H}_{\mathrm{ML}})\,\mathrm{vec}(\delta\hat{H}_{\mathrm{ML}})^H\}\\ &= (\hat{\mathscr{F}}^{-T}\otimes\hat{\mathscr{X}}\hat{\mathscr{F}}^{-1})\mathscr{E}\{\mathrm{vec}(\delta\hat{\mathscr{F}})\,\mathrm{vec}(\delta\hat{\mathscr{F}})^H\}(\hat{\mathscr{F}}^{-*}\otimes\hat{\mathscr{F}}^{-H}\hat{\mathscr{X}}^H)\\ &\quad + (\hat{\mathscr{F}}^{-T}\otimes I_{N_o})\mathscr{E}\{\mathrm{vec}(\delta\hat{\mathscr{X}})\,\mathrm{vec}(\delta\hat{\mathscr{X}})^H\}(\hat{\mathscr{F}}^{-*}\otimes I_{N_o})\\ &\quad - 2\,\mathrm{herm}(\hat{\mathscr{F}}^{-T}\otimes\hat{\mathscr{X}}\hat{\mathscr{F}}^{-1})\mathscr{E}\{\mathrm{vec}(\delta\hat{\mathscr{F}})\,\mathrm{vec}(\delta\hat{\mathscr{X}})^H\}(\hat{\mathscr{F}}^{-*}\otimes I_{N_o})\end{aligned} \tag{26}$$

with $\mathscr{E}$ the Expectation operator, where for example

$$\mathscr{E}\{\mathrm{vec}(\delta\hat{\mathscr{X}})\,\mathrm{vec}(\delta\hat{\mathscr{X}})^H\} = \mathscr{E}\left\{\frac{1}{P}\sum_{k=1}^{P}\mathrm{vec}(\delta X_k)\frac{1}{P}\sum_{l=1}^{P}\mathrm{vec}(\delta X_l)^H\right\} \tag{27}$$

under the assumptions that over the different measurements all signals and noise are stationary and the noise is not correlated, reduces to

$$\mathscr{E}\{\mathrm{vec}(\delta\hat{\mathscr{X}})\,\mathrm{vec}(\delta\hat{\mathscr{X}})^H\} = \frac{1}{P}(I_{N_i}\otimes C_{\mathscr{X}}). \tag{28}$$

Consequently, the expression for the covariance matrix becomes

$$\mathrm{Cov}(\hat{H}_{\mathrm{ML}}) = \frac{1}{P}(\hat{\mathscr{F}}^{-T}\hat{\mathscr{F}}^{-*}) \otimes C_{\mathscr{X}} + \frac{1}{P}(\hat{\mathscr{F}}^{-T}\hat{\mathscr{F}}^{-*}) \otimes (\hat{\mathscr{X}}\hat{\mathscr{F}}^{-1} C_{\mathscr{F}} \hat{\mathscr{F}}^{-H}\hat{\mathscr{X}}^{H}) - \frac{1}{P}(\hat{\mathscr{F}}^{-T}\hat{\mathscr{F}}^{-*}) \otimes (\hat{\mathscr{X}}\hat{\mathscr{F}}^{-1}\mathrm{Cov}(\mathscr{F},\mathscr{X})) - \frac{1}{P}(\hat{\mathscr{F}}^{-T}\hat{\mathscr{F}}^{-*}) \otimes (\mathrm{Cov}(\mathscr{X},\mathscr{F})\hat{\mathscr{F}}^{-H}\hat{\mathscr{X}}^{H})$$

which, given Eq. (23), finally results in

$$\mathrm{Cov}(\hat{H}_{\mathrm{ML}}) = \frac{1}{P}\left[\left(\frac{1}{P}\sum_{k=1}^{P} F_k\right)^{*}\left(\frac{1}{P}\sum_{l=1}^{P} F_l\right)^{T}\right]^{-1} \otimes C_{\varepsilon} \tag{29}$$

with

$$C_{\varepsilon} = \hat{B} C_{\mathscr{D}} \hat{B}^{H}, \quad \hat{B} = [\hat{H}_{\mathrm{ML}}, -I_{N_o}]. \tag{30}$$

Appendix C. Proof for D-optimal experiment design

Lemma 1. *The determinant of $N \times N$ matrices $A^{(i)}$, $i = 1, \ldots, 2^{N^2}$, consisting of only* 1's *and* -1's *can only be equal to $-\alpha$, 0 or α, where $\alpha = 2^{N-1}$.*

Proof. If $A^{(j)}$ is singular then $\det(A^{(j)}) = 0$. On the other hand, if $A^{(j)}$ is regular, it has a determinant $\alpha \neq 0$. Note that all regular matrices $A^{(i)}$ can be derived from $A^{(j)}$ by means of column and row permutations, and multiplications of columns or rows with -1. These operations can only modify the sign of the determinant so that $|\det(A^{(i)})| = \alpha, \forall$ regular matrices $A^{(i)}$. Consider the regular $N \times N$ matrix A_N constructed by making all lower triangular elements including the diagonal ones equal to 1, while the upper triangular elements equal -1. For example

$$A_4 = \begin{bmatrix} 1 & -1 & -1 & -1 \\ 1 & 1 & -1 & -1 \\ 1 & 1 & 1 & -1 \\ 1 & 1 & 1 & 1 \end{bmatrix}. \tag{31}$$

By means of linear column manipulations, it follows that $\det(A_N) = \det(B_N)$ where B_N stands for A_N but with all entries (i,j) where $j > i+1$ equal to 0. For example

$$\det(A_4) = \begin{vmatrix} 1 & -1 & -1 & -1 \\ 1 & 1 & -1 & -1 \\ 1 & 1 & 1 & -1 \\ 1 & 1 & 1 & 1 \end{vmatrix} = \begin{vmatrix} 1 & -1 & 0 & 0 \\ 1 & 1 & -1 & 0 \\ 1 & 1 & 1 & -1 \\ 1 & 1 & 1 & 1 \end{vmatrix} = \det(B_4). \tag{32}$$

Expanding with respect to the first row gives

$$\det(B_4) = \begin{vmatrix} 1 & -1 & 0 & 0 \\ 1 & 1 & -1 & 0 \\ 1 & 1 & 1 & -1 \\ 1 & 1 & 1 & 1 \end{vmatrix} = 1\begin{vmatrix} 1 & -1 & -1 \\ 1 & 1 & -1 \\ 1 & 1 & 1 \end{vmatrix} - (-1)\begin{vmatrix} 1 & -1 & -1 \\ 1 & 1 & -1 \\ 1 & 1 & 1 \end{vmatrix}. \tag{33}$$

From this example it follows that $\det(B_4) = 2\det(A_3) = 2\det(B_3) = 2^2\det(A_2) = 2^3$, and by induction $\det(A_N) = 2^{N-1}$. Thus, $\alpha = 2^{N-1}$. □

Lemma 2. *Consider the convex hull $\mathbf{Q} = \mathbf{Co}\{Q^{(1)}, Q^{(2)}, \ldots, Q^{(2^{N_i^2})}\}$ in the space $\mathbf{R}^{N_i \times N_i}$, supported by all matrices $Q^{(n)} \in \{1, -1\}^{N_i \times N_i}$, $n = 1, \ldots, 2^{N_i^2}$, consisting of only* 1's *and* -1's. *Then, $|\det(Q)|$ with $Q \in \mathbf{Q} = [-1, 1]^{N_i \times N_i}$ (i.e. the set of all $N_i \times N_i$ matrices with entries in the interval $[-1, 1]$), reaches its maximum value in all regular vertex matrices $Q^{(n)}$ of the convex polytope $\mathbf{Q}$.*

Proof. Firstly, it is shown that the maximum value is reached on the boundary $\partial\mathbf{Q}$ of the convex hull $\mathbf{Q}$. Indeed, if Q_* is a point interior to $\mathbf{Q}$ then there exists an $\alpha>1$ such that $\alpha Q_* \in \partial\mathbf{Q}$ and if $\det(\alpha Q_*)\neq 0$ then $|\det(\alpha Q_*)| = |\alpha^{N_i}\det(Q_*)| > |\det(Q_*)|$. The second part of the proof consists in showing that $|\det(Q^{(i)})| \in \{0, A\}, \forall$ vertices $Q^{(i)}$ of the polytope $\mathbf{Q}$. If Q^* is a non-regular vertex matrix then $|\det(Q^*)| = 0$. On the other hand, if Q^* is regular then $|\det(Q^{(i)})|$ equals some value $A>0$. Note that all regular vertex matrices of $\mathbf{Q}$ can be derived from Q^* by means of column and row permutations, and multiplications of columns or rows with -1. These operations can only modify the sign of the determinant so that $|\det(Q^{(i)})| = A, \forall$ regular vertices $Q^{(i)}$ of $\mathbf{Q}$. Eventually, it is shown that for $Q^* \in \partial\mathbf{Q}$, $|\det(Q^*)|$ cannot exceed the value A, obtained in the regular vertex matrices. Assume therefore that there exist a matrix $Q^* \in \partial\mathbf{Q}$ with determinant equal to A and with at least one entry different from 1 or -1. Assume for example that Q^*_{11} is such an entry. The determinant of Q^* can be written as $\det(Q^*) = \sum_{j=1}^{N_i}(-1)^{j+1}Q^*_{1j}\det(Q^*_{(-1,-j)})$ where $Q^*_{(-1,-j)}$ is an (N_i-1)-by-(N_i-1) matrix obtained by deleting the first row and the jth column of Q^*. If Q^*_{11} differs from 0, then it would be possible to exceed A in a vertex which contradicts with our prior result. So, $|Q^*_{11}|$ must equal 1 in the extremum. Otherwise, if $Q^*_{(-1,-1)}$ equals 0, then the value of Q^*_{11} does not matter. □

References

[1] J. Schoukens, R. Pintelon, E. Van der Auderaa, J. Renneboog, Survey of excitation signals for FFT based signal analyzers, *IEEE Transactions on Instrumentation and Measurement* 37 (1988) 342–351.

[2] J. Leuridan, D. De Vis, H. Van Der Auweraer, F. Lembregts, A comparison of some frequency response measurements techniques, in: *Proceedings of the Fourth International Modal Analysis Conference*, 1986.

[3] J.S. Bendat, A.G. Piersol, *Engineering Applications of Correlation and Spectral Analysis*, Wiley, New York, 1980.

[4] P.A.N. Briggs, K.R. Godfrey, Pseudorandom signals for the dynamic analysis of multivariable systems, *Proceedings of the IEE* 113 (7) (1966) 1259–1267.

[5] J. Schoukens, P. Guillaume, R. Pintelon, Design of broadband excitation signals, in: K. Godfrey (Ed.), *Perturbation Signals for System Identification*, Prentice-Hall International Series in Acoustics, Speech and Signal Processing, Prentice-Hall, New York, 1993 (Chapter 3, pp. 126–160).

[6] R. Pintelon, J. Schoukens, Measurement and modeling of linear systems in the presence of nonlinear distortions, in: *Proceedings of the ISMA25 International Conference on Noise and Vibration Engineering*, K.U. Leuven, Leuven, Belgium, September 2000, pp. 451–458.

[7] J. Schoukens, R. Pintelon, Y. Rolain, T. Dobrowiecki, Frequency response measurements in the presence of nonlinear distorsions. A general framework and practical advices, in: *Proceedings of the ISMA25 International Conference on Noise and Vibration Engineering*, K.U. Leuven, Leuven, Belgium, September 2000, pp. 459–464.

[8] J. Schoukens, Y. Rolain, J. Swevers, J. De Cuyper, Simple methods and insights to deal with nonlinear distortions in frf-measurements, *Mechanical Systems and Signal Processing* 14 (4) (2000) 657–666.

[9] J. Schoukens, R. Pintelon, Y. Rolain, T. Dobrowiecki, Frequency response function measurements in the presence of nonlinear distortions, *Automatica* 37 (2001) 939–946.

[10] J. Schoukens, J. Swevers, R. Pintelon, H. Van der Auweraer, Excitation design for frf measurements in the presence of nonlinear distortions, in: *Proceedings of ISMA 2002*, *International Conference on Noise and Vibration Engineering*, K.U. Leuven, Leuven, Belgium, September 2002, pp. 951–957.

[11] S.A. Billings, K.M. Tsang, Spectral analysis for nonlinear systems, part I: parametric nonlinear spectral analysis, *Mechanical Systems and Signal Processing* 3 (4) (1989) 319–340.

[12] S.A. Billings, K.M. Tsang, Spectral analysis for nonlinear systems, part II: interpretation of nonlinear frequency response functions, *Mechanical Systems and Signal Processing* 3 (4) (1989) 341–359.

[13] S.A. Billings, K.M. Tsang, G.R. Tomlinson, Spectral analysis for nonlinear systems, part III: case study examples, *Mechanical Systems and Signal Processing* 4 (1) (1990) 3–21.

[14] J. Schoukens, R. Pintelon, Y. Rolain, Broadband versus stepped sine FRF measurements, *IEEE Transactions on Instrumentation and Measurement* 49 (2) (2000) 275–278.

[15] D.R. Brillinger, *Time Series*: *Data Analysis and Theory*, McGraw-Hill, New York, expanded edition, 1981.

[16] B.D.O. Anderson, Identification of scalar errors-in-variables models with dynamics, *Automatica* 21 (6) (1985) 709–716.

[17] L. Ljung, System identification: theory for the user, *Prentice-Hall Information and System Sciences Series*, Prentice-Hall, Englewood Cliffs, NJ, 1987.

[18] T. Söderström, P. Stoica, *System Identification*, Printice-Hall, New York, 1989.

[19] P. Verboven, Frequency-domain system identification for modal analysis, Ph.D. Thesis, Vrije Universiteit Brussel, Belgium, May 2002.

[20] S. Van Huffel, J. Vandewalle, The total least squares problem: computational aspects and analysis, *Frontiers in Applied Mathematics*, Vol. 9, SIAM, Philadelphia, PA, 1991.

[21] M. Kendall, A. Stuart, Inference and relationship, *The Advanced Theory of Statistics*, Vol. 2, fourth edition, Charles Griffin & Company Limited, London, 1979.

[22] L.J. Gleser, Estimation in a multivariable 'errors-in-variables' regression model: large sample results, *The Annals of Statistics* 9 (1) (1981) 24–44.
[23] W.A. Fuller, *Measurement Error Models*, Wiley, New York, 1987.
[24] P. Verboven, P. Guillaume, M. Van Overmeire, Improved modal parameter identification by non-parametric modeling of the measurement noise, in: *Proceedings of the 17th International Modal Analysis Conference*, Kissimmee, FL, USA, February 8–11 1999, pp. 1984–1990.
[25] P. Guillaume, R. Pintelon, J. Schoukens, Accurate estimation of multivariable frequency response functions, in: *Proceedings of the 1996 Triennial World Congress of IFAC*, Vol. 1, San Francisco, July 1–5 1996, pp. 423–428.
[26] R. Pintelon, J. Schoukens, *System Identification: A Frequency Domain Approach*, IEEE Press, New Jersey, USA, 2001.
[27] P. Guillaume, R. Pintelon, J. Schoukens, Nonparametric frequency response function estimators based on nonlinear averaging techniques, *IEEE Transactions on Instrumentation and Measurement* 41 (6) (1992) 739–746.
[28] P. Guillaume, Frequency response measurements of multivariable systems using nonlinear averaging techniques, *IEEE Transactions on Instrumentation and Measurement* 47 (3) (1998) 796–800.
[29] J. Schoukens, Y. Rolain, G. Simon, R. Pintelon, Fully automated spectral analysis of periodic signals, in: *Proceedings of the IEEE Instrumentation and Measurement Technology Conference*, Anchorage, AK, USA, 2002.
[30] M.R. Schroeder, Synthesis of low-peak signals and binary sequences with low autocorrelation, *IEEE Transactions on Information Theory* 16 (1) (1970) 85–89.
[31] E. Van der Auderaa, J. Schoukens, J. Renneboog, Peak factor minimization using a time-frequency domain swapping algorithm, *IEEE Transactions on Instrumentation and Measurement* 37 (1988) 145–147.
[32] P. Guillaume, J. Schoukens, R. Pintelon, I. Kollár, Crest-factor minimization using nonlinear Chebyshev approximation methods, *IEEE Transactions on Instrumentation and Measurement* 40 (6) (1991) 982–989.
[33] G. Simon, J. Schoukens, Robust broadband periodic excitation design, *IEEE Transactions on Instrumentation and Measurement* 49 (2) (2000) 270–274.
[34] P. Guillaume, R. Pintelon, J. Schoukens, Parametric identification of two-port models in the frequency domain, *IEEE Transactions on Instrumentation and Measurement* 41 (2) (1992) 233–239.
[35] P. Guillaume, I. Kollár, J. Schoukens, On the design of optimal input signals for multi-input, multi-output system identification, in: *Proceedings of the ISMA15 International Conference on Noise and Vibration Engineering*, Leuven, September 19–21, 1990, pp. 1223–1239.
[36] R.J. Allemang, R.W. Rost, D.L. Brown, Multiple input estimation of frequency response functions: excitation considerations, *The American Society of Mechanical Engineers* 83-DET-73 (1983) 1–11.
[37] V.V. Fedorov, *Theory of Optimal Experiments*, Academic Press, New York, 1972.